UWB Printed MIMO Antennas for Satellite Sensing System (SRSS) Applications

Wyssem Fathallah[1], Chafai Abdelhamid[2], Chokri Baccouch[3], Alsharef Mohammad[4], Khalil Jouili[5], Hedi Sakli [6]*
SYS'COM Laboratory LR99ES21, National Engineering School of Tunis, Tunis El Manar University, Tunis, 1002, Tunisia[1, 3]
MACS Research Laboratory RL16ES22, National Engineering School of Gabes, Gabes University, Gabes, 6029, Tunisia[2, 6]
Department of Electrical Engineering, College of Engineering, Taif University, Taif, Saudi Arabia[4]
Laboratory of Advanced Systems, Polytechnic School of Tunisia (EPT), Marsa, 2078, Tunisia[5]
EITA Consulting, 7 Rue du Chant des oiseaux, 78360 Montesson, France[6]

***Abstract*—The deployment of ultra-wideband (UWB) technology offers enhanced capabilities for various Internet of Things (IoT) applications, including smart cities, smart buildings, smart aggregation, and smart healthcare. UWB technology supports high data rate communication over short distances with very low power densities. This paper presents a UWB printed antenna design with multiple input and output (MIMO) capabilities, specifically tailored for Routed Satellite Sensor Systems (SRSS) to enhance IoT applications. The proposed UWB printed antenna, designed for the 2–18 GHz frequency band, has overall dimensions of 14.5 mm x 14.5 mm, with an efficiency exceeding 70% and a gain ranging from 2 to 6.5 dB. Both simulated and measured reflection parameters (|S11|) at the antenna input show strong agreement. Furthermore, a compact MIMO system is introduced, featuring four closely spaced antennas with a gap of 0.03λ, housed in a 60 mm x 48 mm module. To minimize coupling effects between the antennas, the design incorporates five Split Ring Resonator (SRR) elements arranged linearly between the radiating elements. This arrangement achieves a mutual coupling reduction to -35 dB at 8 GHz, compared to -20 dB isolation in systems without SRR. The results demonstrate that the proposed MIMO antenna system offers promising performance and meets the requirements for effective space communication within satellite sensor networks.**

***Keywords*—5G antenna; 5G satellite networks; millimeter band; wireless communications; SRR; IoT**

I. Introduction

UWB technology was originally developed for military applications but began to be used in civilian applications. Arousing growing interest within the scientific and industrial community, it was transferred to telecommunications applications [1-12]. This technology is used in other applications, such as structural health monitoring (SHM) for large structures, and in particular in the aeronautics and space fields are under development [13].

Other applications of wireless sensor networks operating using UWB spectrums appear in smart homes, the biomedical field, natural disaster detection, intrusion detection, pollutant detection, agriculture, and many other fields [14]. They provide great ease of use and reduce the cost and time of deployment. One can't talk about UWB without mentioning Internet of Things (IoT), the concept of connected devices, continues to show promising progress, and now, with the re-emergence of UWB technology, IoT devices that require location and movement data are performing better than ever for the cost and time of deployment [15]. Thanks to UWB interoperability, this communication protocol can be used to take advantage of smart technologies such as Bluetooth, WiFi, and the IoT's. UWB can play a key role in redesigning the IoT devices already available and in introducing more sophisticated networks of interconnected devices in the future [16]. In wireless communication systems, antennas play a very important role as it is the backbone of any wirelessly communicating system. To meet the emerging requirements of the smart IoT devices an enhanced performance antenna is required [17]. Moreover, to meet the requirements of the MIMO system a compact yet low mutual coupling antenna has become essential for communication systems.

Thus, the researcher puts a lot of effort to design compact size UWB antenna for IoT devices [18–28]. For instance, a metamaterial inspired circular split ring resonator shaped antenna is designed for UWB application in study [18]. Although the antenna offers a UWB operational band with a notch band ranges 7 – 8 GHz it had a setback of bigger dimension along with lower cutoff frequency around 3.4 GHz. In study [19] a dual stub loaded antenna having dual reconfigurable notch band is proposed for UWB applications. However, the insertion of the diodes and biasing circuit causes the degrading of antenna performance resulting in a low gain throughout the band of interest. Likewise, in [20] a rectangular monopole antenna exhibiting broad bandwidth is converted into a UWB antenna by initially modifying the ground plane, then by truncating the radiating structure and finally loading some parasitic elements. The resulting antenna offers UWB ranges 2.5–18 GHz at the cost of complex structure along with low gain and large physical size. The study in [21– 22] present the conversation of circular and semi-circular monopole antenna into UWB antenna by truncating the radiating structure along with ground plane. Resistor loaded anti-spiral shaped UWB antenna is presented in [24], where flexible antenna is designed by compromising the size of antenna along with partial covering the UWB spectrum. Moreover, the work reported in study [26–28] has a relatively big size as compared to other literary works. Furthermore, none of the discussed can be used for IoT applications due to their SISO nature.

Considering the requirements of IoT and future networks that require MIMO antenna, there is a dire need to design UWB MIMO antenna with low mutual coupling in study [29–35]. A

compact size two-port UWB antenna is presented in study [29] where two open ended stubs are loaded, and their structure is modified to achieve a mutual coupling of -15 dB between adjacent elements. On the other hand, a truncated corner shaped UWB antenna is utilized to design a 4-element UWB MIMO antenna. The antenna elements are placed orthogonal to each other to achieve low mutual coupling along with defected ground structure to further reduce the mutual coupling to < -20 dB. A flower shaped semi-fractal antenna is proposed in study [31], which is converted into 4-element MIMO antenna. Four-open ended stubs were loaded to reduce the mutual coupling among MIMO elements; however, the MIMO antenna system only offers the mutual coupling of < -18 dB. Likewise, in study [32] a hollow ground plane and inverted L-shaped stub loaded UWB MIMO antenna is presented. The antenna offers UWB ranges 2.84 – 15.88 GHz having a overall size of 58 x 58 mm2 along with a setback of high mutual coupling. Another MIMO antenna for UWB application is proposed in study [33] in which the orthogonal placement of MIMO element is utilized to achieve a low mutual coupling while compromising the overall size of antenna. A tapered-fed circular shaped MIMO antenna is designed for UWB applications while neutralization lines along with DGS and inverted L-shaped open stubs are utilized to reduce the mutual coupling [34]. On the other hand, a pair of C-shaped parasitic patches are loaded at the back of antenna to reduce the mutual coupling [35]. However, both the works have the disadvantage of bigger size along with complex geometrical structure.

All of the aforementioned works either lack in covering complete UWB spectrum or have large physical dimension along with most of them suffering from complex geometrical structure. Therefore, this study focuses on the design of geometrically simple yet UWB MIMO antenna having low mutual coupling along with high gain is given in Section II. The antenna design methodology is discussed in Section III, afterward the results will be discussed in Section IV, and the manuscript is concluded in Section V.

II. Antenna Design

The design methodology started from designing a conventional rectangular patch antenna that resonates at central frequency of 10 GHz, as depicted in Fig. 1. The length and width of the rectangular patch along with microstrip feedline can be estimated using the equations provided in [36]. The setback of conventional microstrip antenna, the narrow bandwidth, is nullified using the partial ground plane technique along with truncated corners, as shown in Fig. 1 (a). This helps in achieving a broad |S11| < -10dB impedance bandwidth ranging 4–9.5 GHz, as illustrated in Fig. 1(b). Although there is significant improvement observed in bandwidth, still the antenna didn't cover the entire UWB spectrum ranges 3-10.3 GHz. Therefore, to further improve the performance of the antenna another iteration is performed by truncating the lower corners of radiators along with implementing the DGS, as shown in Fig. 1(a). After optimizing the results, the antenna again offers wide operational bandwidth ranges 5–15.7 GHz, as shown in Fig. 1(b). It is important to note here that although the bandwidth of the antenna increases but operational spectrum shifted toward higher frequency.

Thus, there is need to shift the lower end of the resonating band. For said purpose two u-shaped slots were utilized, they are etched from the radiator and by optimizing the parameters of the slots the antenna resonance can be shifted toward lower side. The other parameters of the proposed antenna are also optimized which results in UWB spectrum ranges 2 – 18 GHz, covering UWB, extended UWB and Ku-band, as shown in Fig. 1(b).

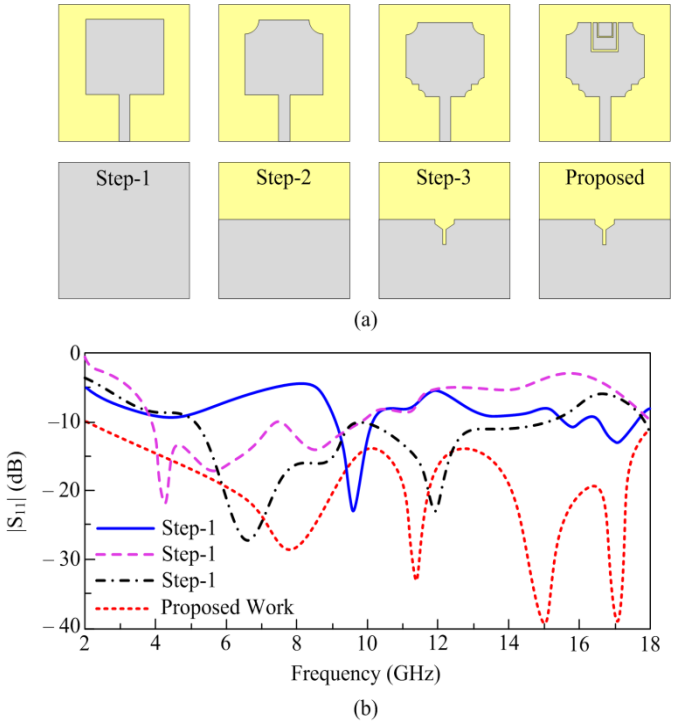

Fig. 1. (a) Geometrical configuration (b) Reflection coefficient of various modifications in radiator and ground plane.

Fig. 2 depicts the geometrical configuration of the proposed ultra-wideband antenna, while Table I summarizes the optimal parameters obtained by simulation.

For in-depth understanding of UWB behavior of antenna, Fig. 3 depicts the impedance characteristics of the antenna. It can be observed that the proposed antenna offers real impedance value around 50 Ω while the imaginary value stays around 0 Ω which also proves the ultra-wideband behaviour of the antenna.

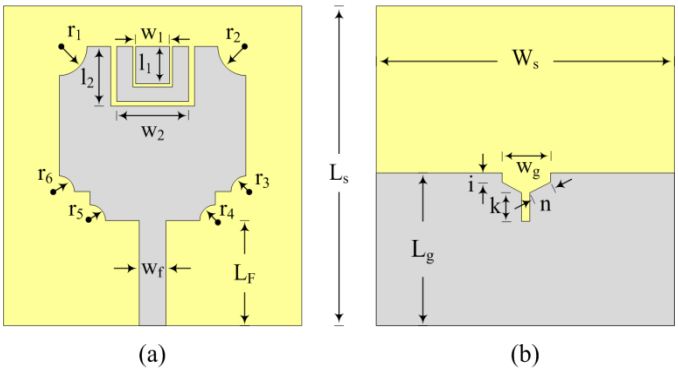

Fig. 2. Final geometry of the proposed antenna: (a) the front view, (b) backside view.

TABLE I. PROPOSED ANTENNA DIMENSIONS IN DETAIL

Elements	*Parameters*	*Values(mm)*
Patch	$r_1=r_2$	2.5
	W_1	3.4
	L_1	7.5
	$r_3=r_4=r_5=r_6$	1.5
	W_3	6.17
	L_f	13.5
	W_f	3
	W_2	7.2
	F	0.3
Dielectric substrate	W_s	25
	L_s	30
	H_s	1.6
	ε_r	4.4
Ground Plane	L_g	12.5
	W_g	3.5
	n	2.4
	i	0.75
	k	2.3

The gain of the proposed UWB antenna is shown in Fig. 4. The antenna offers a minimum gain of 2.4 dB around 2 GHz, it tends to start increasing for higher frequency and reach up to the maximum value of 5.8 dB around 17.7 GHz. Thus, the gain results strength the potential of the proposed work for UWB and Ku-band applications.

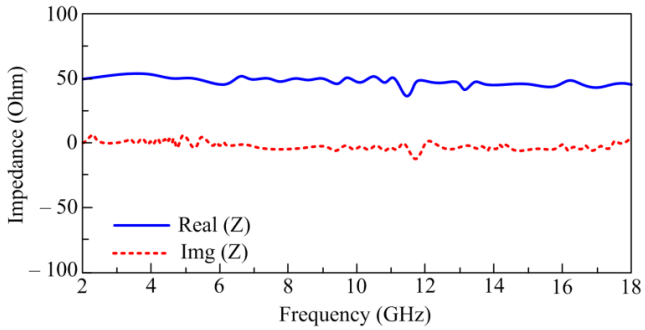

Fig. 3. Proposed antenna impedance characteristics.

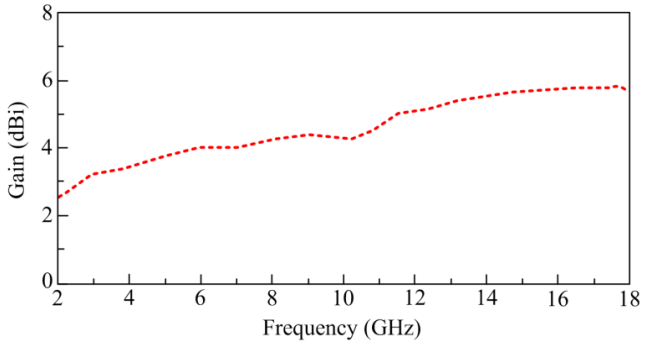

Fig. 4. Peak gain of proposed work.

The radiation pattern of the proposed antenna at the selected frequencies of 8 and 15 GHz is shown in Fig. 5. The antenna offers a nearly omni directional radiation pattern in E-plane for both selected frequencies, while for H-plane the antenna offers a dual beam like structure. Moreover, Fig. 6 illustrates the radiation efficiency in the operational band, where antenna offers a minimum efficiency of 80% throughout the band of interest.

The distribution of the current at 8 GHz and 15 GHz of the proposed antenna is shown in Fig. 7. It can be seen that additional paths for surface currents are formed when slits are present. This results in a second resonance, increasing the bandwidth.

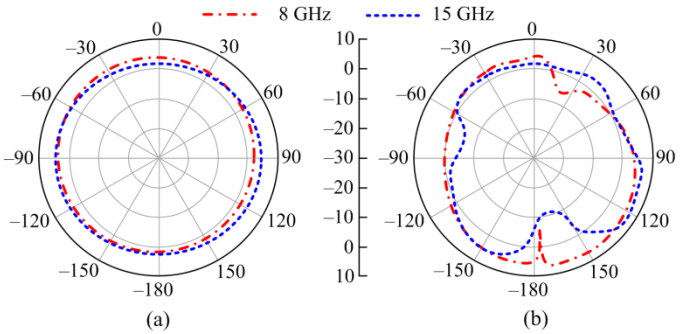

Fig. 5. Radiation pattern of proposed antenna in (a) E-plane and (b) H-plane.

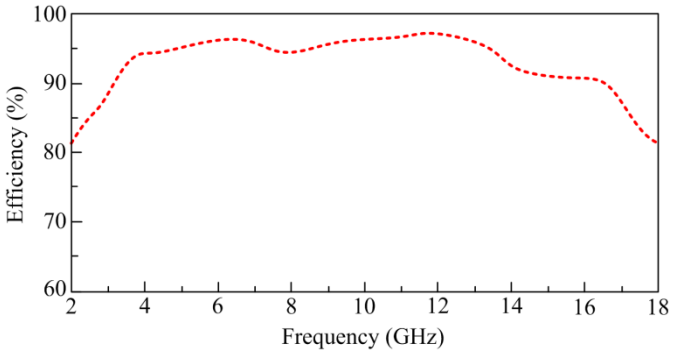

Fig. 6. Efficiency variation of proposed work.

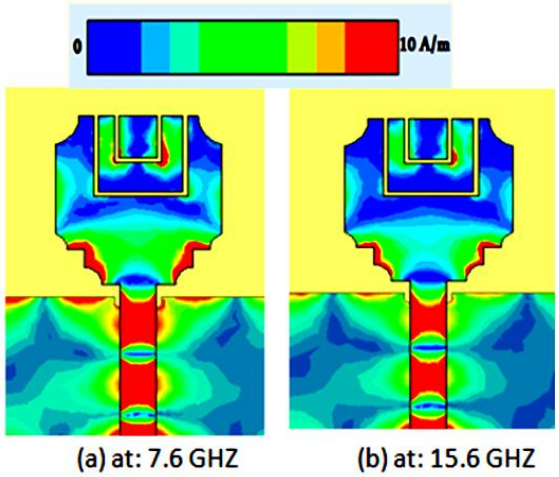

Fig. 7. Current distribution of proposed UWB antenna.

To validate the various performance parameters of the proposed UWB antenna a sample prototype is fabricated and later used for measurements, as shown in Fig. 8. Various parameters including |S11| and radiation pattern were measured and compared with simulated results. The comparison among estimated and measured |S11| results of proposed UWB antenna is shown in Fig. 9. A strong comparison among both results is found having identical wideband operation, a little deviation is observed in values of return loss which may be due to inaccuracy of measurement setup or due to fabrication tolerance.

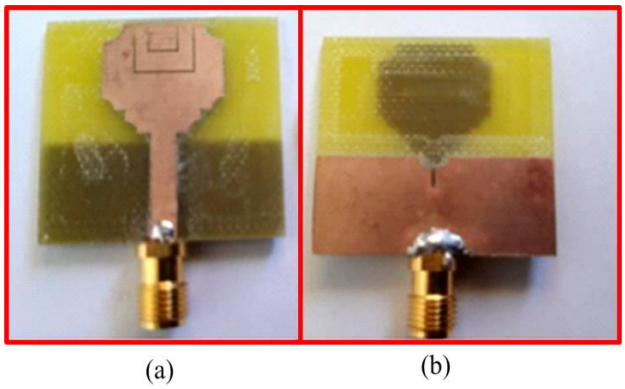

Fig. 8. Fabricated Antenna: (a) Top view and (b) Bottom view.

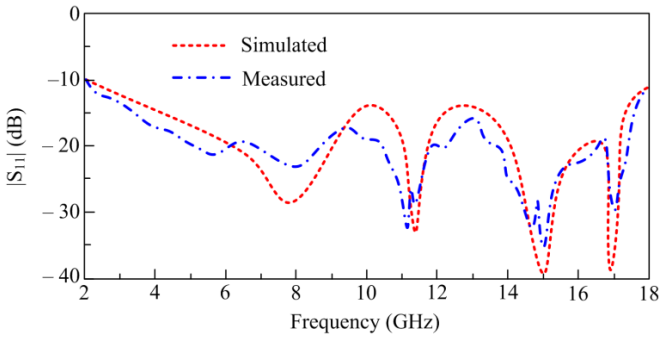

Fig. 9. Comparison of reflection coefficient among simulated and measured results.

For the selected frequency of 8 GHz, the comparison among the radiation patterns found using the EM tool and measurement is presented in Fig. 10. A strong correlation is observed, with nearly identical patterns in both cases. Thus, in terms of all performance parameters, strong results are observed among the simulated and measured values, which illustrates the performance stability of the proposed antenna.

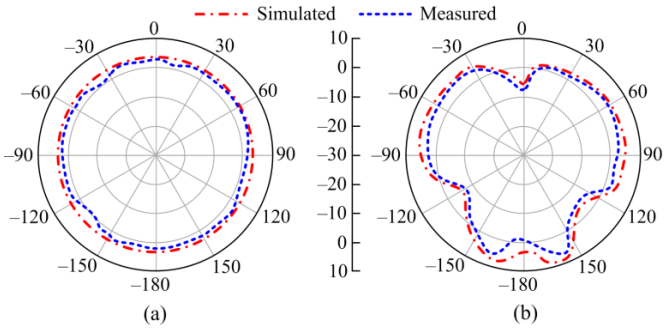

Fig. 10. Radiation pattern at 8 GHz: (a) E-plane and (b) H-plane.

III. Common Techniques to Reduce Mutual Coupling among MIMO Antenna Elements

Diversity and MIMO systems require good isolation between antennas. Much research has been done over the years to find techniques to reduce mutual coupling and increase isolation between antenna elements. In this part, a short explanation of various major techniques is done to better understand the working and then utilized a combination of them to reduce mutual coupling of proposed MIMO antenna system.

A. Structural Change of Ground Plane

This method is well known as DGS and consists of modifying the structure of the ground plane to change the current distribution [37]. MIMO systems use the effect of notch filters to minimize mutual coupling between radiating elements. In fact, a common use of the DGS method is to insert a slot in the ground plane [38]. The DGS solution is very easy to implement because its operation depends on the resonant frequency and not on the antenna type. However, the main drawback of this method is mainly integration issues on mobile phones.

B. Use of EBG (Electromagnetic Band Gap) Structure

Generally, in antenna decoupling, the EBG structure is similar to a notch filter [39]. In fact, a typical EBG cell has a mushroom-shaped structure containing patches and grounded vias. Moreover, the EBG structure can be used as a magnetic wall through which the phase of the reflection coefficient becomes zero for an incident wave. Therefore, surface wave propagation will be suppressed [40]. On the other hand, this method requires considerable space, especially for low frequencies [41]. Moreover, this solution is not commonly used in practice due to its complexity and large size [42]. In study [43], four rows of fork-shaped EBG patches were inserted between the E-plane coupling antennas to reduce mutual coupling. A mutual coupling reduction of 6.51 dB was achieved at 5.2 GHz when using the EBG structure.

C. Use of the Neutralization Line

This approach is generally used to ensure better isolation between two PIFA (Planar Inverted-F Antenna) antennas [44]. Indeed, it is a question of introducing a simple suspended metal line, integrated between the power supplies or the short circuits of the PIFA antennas. In addition, the neutralization line supports strong currents so that the direction of the current is radiated towards the antenna itself and not towards the power connector of the second antenna. It is also possible to cut all path couplings (OTA (over the air) couplings and ground plane power couplings) by changing the dimensions of the neutralization lines. For example, in study [45], the authors inserted an interrupted neutralization wire physically connected to two PIFA elements (operating in the UMTS band of 1920–2170 MHz).

The introduction of neutralizing lines was used to cancel pre-existing mutual coupling. This is because the line stores a certain amount of current that is fed from one antenna element to the other. In other words, the antenna achieved less than -18 dB of mutual coupling at a frequency of 2 GHz because an additional path was created to compensate for the antenna-to-antenna current on the circuit board. Recently, a new print diversity monopole antenna for WiFi and WiMAX applications was

presented in study [46]. It's based on the same concept, but with a much more complex kill line integration. The antenna consists of two crescent-shaped radiators placed symmetrically about a faulty ground plane, with neutralizing lines to achieve a bandwidth of 2.4 to 4.2 GHz and mutual coupling of less than -17 dB connected between them.

D. Using an Isolation Network

This method aims to reduce the mutual impedance or transmission coefficient between the radiating elements to zero while maintaining good impedance matching in each element [47]. In the literature, we have found various antenna array configurations based on 180° hybrid couplers or RF switches.

E. Use of Parasitic Resonators

This is similar to neutralizing wire-based solutions in that the parasitic resonator is integrated in the middle of the two antennas to minimize mutual coupling between them. In other words, this solution artificially creates an additional coupling path between antennas. However, simply changing the spacing between the radiating elements requires changing the structure of the resonator to ensure good isolation. This limitation then hinders the serial application of the parasitic resonator [48].

Although the above solutions overcome the coupling effect between the antennas, there are other innovative and more efficient means. In fact, recently, the development of metamaterials to design and optimize antenna characteristics has shown great importance, not only to minimize antenna size, but also to provide better isolation and reduce the spacing between elements radiating [49].

At this stage of our research, part of the solutions developed within the framework of the study of multi-antenna systems intended for wireless communications or intended to be used in applications of the diversity or MIMO type have been presented [50-53]. These solutions have been investigated with the aim of covering several wireless communication standards and improving the isolation between the antennas that make up these systems. Consequently, having antennas very close to each other and operating in neighboring or even identical frequency bands is an ever-present challenge because communication systems must have increasingly new, numerous, and innovative functionalities.

In the proposed study the EBG structure along with DGS is utilized to reduce the mutual coupling and explain in forthcoming sections.

IV. Results and Discussions

Increasing the number of transmit and receive antennas without increasing radiated power can improve communication quality and channel capacity. The MIMO antenna design proposed in this article has four identical radiating elements, extracted by already designed unit element, as shown in Fig. 11. The overall dimensions of MIMO antenna system are Lsub × Wsub (60 × 48 mm2), having edge to edge distance between all elements is 5mm, as depicted in Fig. 11.

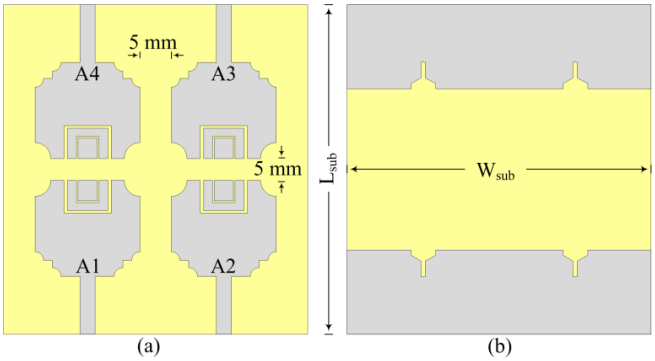

Fig. 11. UWB-MIMO antenna system without decoupling structure.

A. Initial Prototype Simulation Results

The simulated S-parameters of the 4-element MIMO antenna without any decoupling structure are shown in Fig. 12. Due to the symmetry in structure, the S-parameter analysis can be easily performed. The |S11| of the MIMO antenna remain almost identical to the unit element having |S11| < -10dB bandwidth ranges 2–18 GHz. On the other hand the transmission coefficient |Sij|, where i,j=1,2, offers a high value of more than -10 dB. This high value of transmission coefficient is not acceptable for present and future MIMO systems. The easiest way to reduce the value of |Sij| is to increase the edge-to-edge distance, however, it will increase the size of the antenna and thus compactness will vanish.

According to Fig. 13, the surface current circulation in the radiating element is high which leads to strong coupling as already indicated by the high values of |Sij|. Surface currents generated by the excited antenna flow to the other non-excited elements, as shown in Fig. 13.

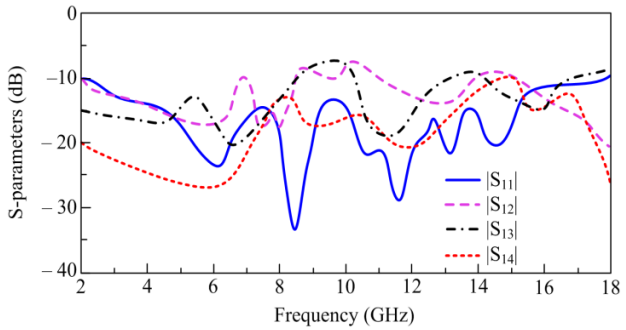

Fig. 12. S-parameters of UWB-MIMO antenna system.

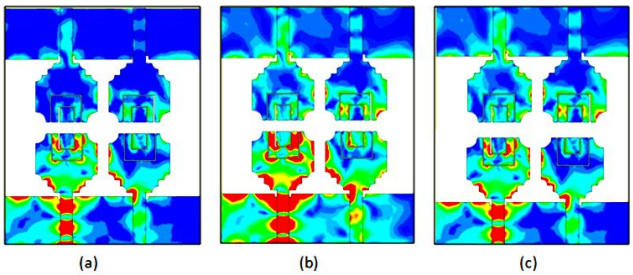

Fig. 13. Effect of the current distribution of antenna 1 on the three other antennas at frequencies: (a) 8 GHz (b) 15 GHz.

Only one element of the MIMO antenna is energized (antenna 1), but we can see currents in the other three components that are not energized. As a result, without excitation, hot spots occur on at least one additional radiating element (2, 3 or 4). Although the maximum current on the unexcited antenna does not equal the maximum current on the excited antenna, it is sufficient to increase coupling between the components. However, compared to the minimum frequency in the operating band (2 GHz), the distance between them is only 0.03λ.

The mutual coupling comes from the capacitive coupling between the radiating elements and the current flowing on the PCB. Because the isolation value obtained is insufficient for a powerful multi-antenna system, thus a more effective way is required to reduce the coupling while leaving the four elements in their original places, i.e., to have a compact size MIMO antenna.

B. Design of SRR Unit Cells

A two small rectangular square split ring resonator (SRR) unit cells operating at frequencies corresponding to well-defined bands WiMAX and X-Band. Afterwards, a rectangular strip is loaded to widen the band of coverage by the SRR unit cell, as shown in Fig. 14.

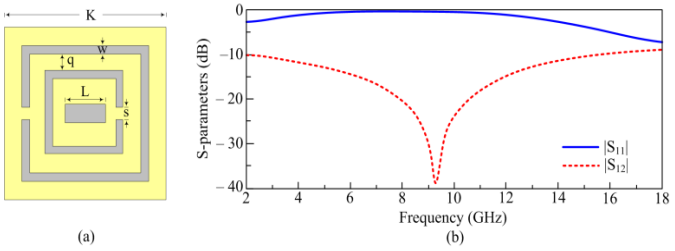

Fig. 14. (a) Geometry of proposed SRR (b) Reflection and transmission coefficients of the proposed SRR.

For ease of understanding the S-parameter-based method is adopted and used to analyze the performance of the Metamaterial unit cell. The designing approach is based on a systematic approach to unit cell design, for this reason, the overall cell size should be smaller than the wavelength (dλ) (approximately λ0/11 in presented case). The geometrical structure along with respective S-parameters is shown in Fig. 14. The unit cell of the metamaterial operates from 2.2–16.7 GHz band, covering almost the entire band offered by proposed unit element of the MIMO antenna. The metamaterial cell is mounted on an FR4 type epoxy dielectric substrate with a dielectric constant of 4.4, a loss factor of 0.02, and a thickness of 1.6mm. This SRR square has an outside side of 2 mm, a track width of 0.2 mm, and a 0.3 mm gap cut on one of these sides. It is two concentric rings with a spacing of 0.15 mm between them and an inner ring measures 1.3 mm on the outside. Before starting the simulation, an electric and magnetic wall was installed in a 2.5 × 2.5 × 5 mm^3 radiation box, these dielectric walls must be used to verify the SRR's requisite excitation conditions. The magnetic field must be positioned along the ring's axis to provide greater magnetic excitation and circulation of the induction current. To do this, two domain walls parallel to the XY- and XZ-plane and an electric wall are provided. The electric field is parallel to OY-axis and the propagation vector is along the OX-axis to ensure a symmetrical current distribution. The optimized dimensions of the unit element are enlisted in Table II.

TABLE II. DIMENSIONS OF SRR UNIT CELL

Parameters	*Values(mm)*
s	0.3
q	0.2
w	0.15
k	2
L	*0.75*

C. Improved Insulation by Loading SRR and DGS

Initially, to improve the separation of this initial structure by known methods based on MTM applied to MIMO systems [54]. Therefore, four chains consisting of five SRR unit elements are inserted between the four excitation-radiating elements of the MIMO system. The UWB MIMO antenna configuration is illustrated in Fig. 15(a), the MIMO antenna design is the same as the previously design MIMO antenna with edge-to-edge gap of 5 mm, except that four strings of SSRs on the top layer of the substrate are added to improve the isolation between the antenna elements, (1-2, 2-3, 3-4 and 1-4). SRRs can act as a reflector and decrease the surface current between antenna elements which consequently reduce the mutual coupling between MIMO antenna elements. Furthermore, a t-shaped like dual slots were also etched in the ground plane which helps in further decrement of mutual coupling between elements placed side by side (1-2, 3-4), as depicted in Fig. 15(b).

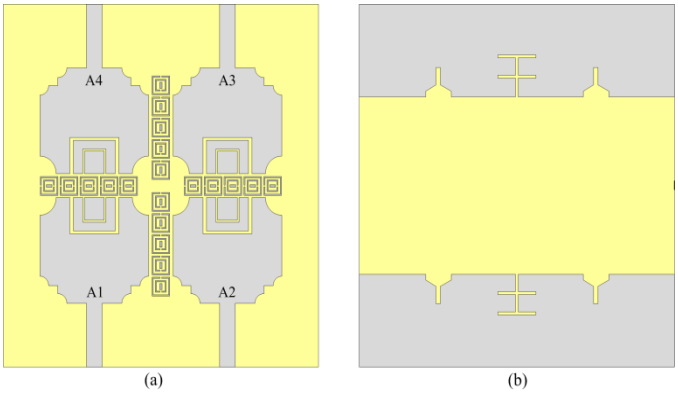

Fig. 15. Proposed four-element MIMO UWB antenna configuration with decoupling network.

A fabricated prototype is used to verify the results of the MIMO antenna loaded with SRR and DGs, as depicted in Fig. 16. Comparison among |S11| of the MIMO antenna loaded with decoupling structure is shown in Fig. 17. It can be observed that a good comparison between simulated and measured results is offered while covering the entire band spectrum globally allocated for UWB and Ku-band applications.

The mutual coupling of the MIMO antenna loaded with decoupling structure is depicted in Fig. 18. The antenna offers a low mutual coupling of less than -20 dB in the entire bandwidth having a good relationship among simulated and measured results.

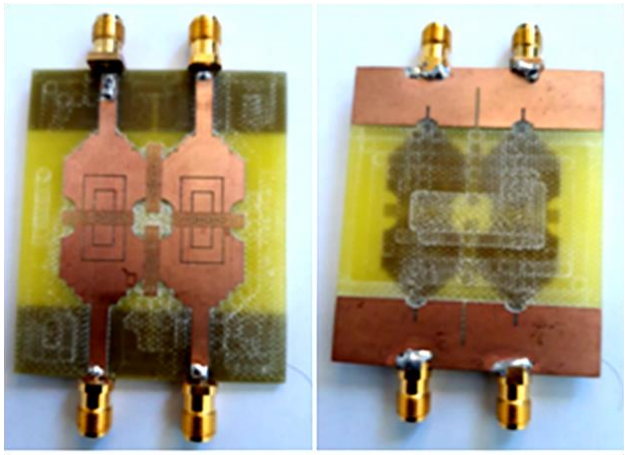

Fig. 16. Manufactured MIMO UWB antenna system with decoupling structure.

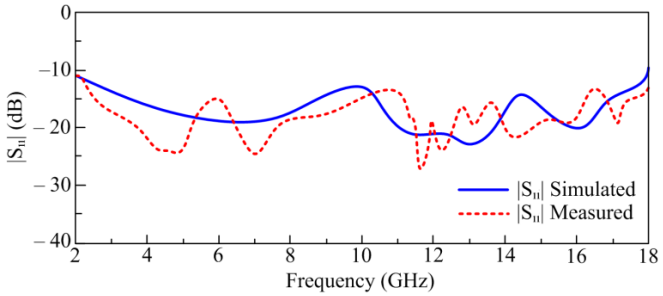

Fig. 17. |S11| of MIMO antenna system with SRRs.

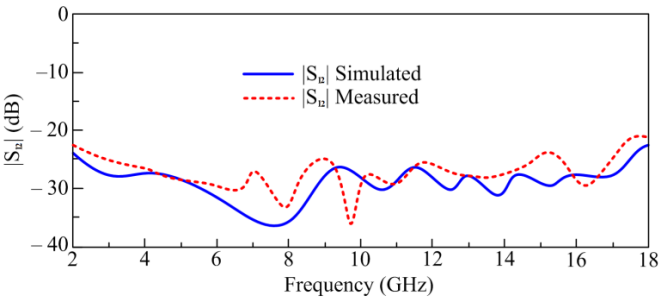

Fig. 18. |S12| (Simulated and measured) of 4-element MIMO UWB antenna system with isolation based on SRRs.

The other performance parameters that characterize the MIMO antenna are the envelope correlation coefficient (ECC) and diversity gain (DG). These parameters are analyzed and their impact on the overall performance of the antenna is considered. As already mentioned, the ECC measures the correlation between the radiating elements. It is also important to note that it is better to have the minimum possible ECC to crystallize the good performance of our MIMO system. In a MIMO system, the signals received must be sufficiently decorrelated to have good diversity. The parameter that describes the independence of the signals is called the correlation envelope. It is zero in the ideal case and must be less than 0.5 in order to obtain good diversity. In a 4-port MIMO system, ECC can be determined between ports 1, 2, 3, and 4 using the expression (1) and (2).

$$ECC = \frac{\left| \iint_{4\pi} (B_i(\theta,\phi)) \times (B_j(\theta,\phi)) d\Omega \right|^2}{\iint_{4\pi} \left|(B_i(\theta,\phi))\right|^2 d\Omega \iint_{4\pi} \left|(B_j(\theta,\phi))\right|^2 d\Omega} \quad (1)$$

Bi(θ, φ) is the 3D radiation pattern when the ith antenna is excited, Bj(θ, φ) is the 3D radiation pattern when the jth antenna is excited, Ω is the solid angle[55].

The disadvantage of this formula is to require a very precise estimation of the radiation patterns and therefore to lead to heavy calculations [56]. Another simplified solution is to calculate the correlation envelope using the S parameters [57]. Therefore, for a system with N antennas, equation (2) allows us to use:

$$ECC = \frac{\left| \sum_{n=1}^{N} S_{i,n}^{*} S_{n,j}^{*} \right|^2}{\prod_{k=i,j} \left[1 - \left| \sum_{n=1}^{N} S_{i,n}^{*} S_{n,j}^{*} \right| \right]} \quad (2)$$

N: Number of antennas, i and j denote antennas i and j

To use this formula (2), it is however necessary to satisfy certain conditions. When one of the antennas is powered, the others are loaded with a reference impedance (usually 50 Ω). The antenna system must be lossless, therefore with very high radiated efficiency [58], and low mutual coupling (< -6 dB).

To ensure that the signal-to-noise ratio (SNR) of the combined signal is better than the signal-to-noise ratio received from a single antenna in a MIMO system, the diversity gain (DG) should also be set to its recommended value should be inspected against value of about 10 dB.

The comparison among simulated and measured ECC and DG is shown in Fig. 19. The ECC offered by proposed work is less than 0.125 while the diversity gain > 9.9 dB is found, as shown in Fig. 19(a) and (b), respectively.

Table III shows a comparison of the UWB MIMO antenna with other existing antennas in the literature for similar applications. It can be observed that work presented in [32 – 33] offers large size as compared to proposed work along with setback of low mutual coupling and high ECC value. On the other hand, although the antenna proposed in [29-31, 34-35] offers a relatively compact size but most of the antennas are 2-port MIMO along with that they have set back of not covering the lower cut off frequency of UWB spectrum and high value of mutual coupling. Thus, it is evident from the comparison with recent works that proposed work offers a good combination of 4-port compact size MIMO antenna having UWB spectrum along with low mutual coupling and ECC values.

TABLE III. COMPARISON OF UWB MIMO ANTENNA

Ref	**Dimensions** *(mm xmm)*	*Element Number*	**Band With (GHz)**	*Mutual Coupling (dB)*	**Gain Range** *(dBi)*	*Radiation Efficiency(%)*	*ECC*
[29]	30 x 18	2	4.3 – 15.6	< -15	2.5 – 5.35	89	< 0.05
[30]	35 x 35	4	3.8 - 15	< -20	3 – 5	Not given	< 0.07
[31]	40 x 40	4	3.1 – 14	< -15	4.4 – 5	70	<0.015
[32]	58 x 58	4	2.84 – 15	< -16	3.5 – 6.35	> 78	< 0.07
[33]	80 x 80	4	3 – 14	< -17	1.2 – 4.8	> 78	< 0.02
[34]	30 x 60	2	2.7 – 20	< -13	3.7 – 6	Not given	< 0.07
[35]	31 x 78	2	3.1 – 13.5	< -17	2 – 4	> 78	< 0.18
Proposed Antenna	60 x 48	4	2-18	< -25	2-6.5	> 90	< 0.0125

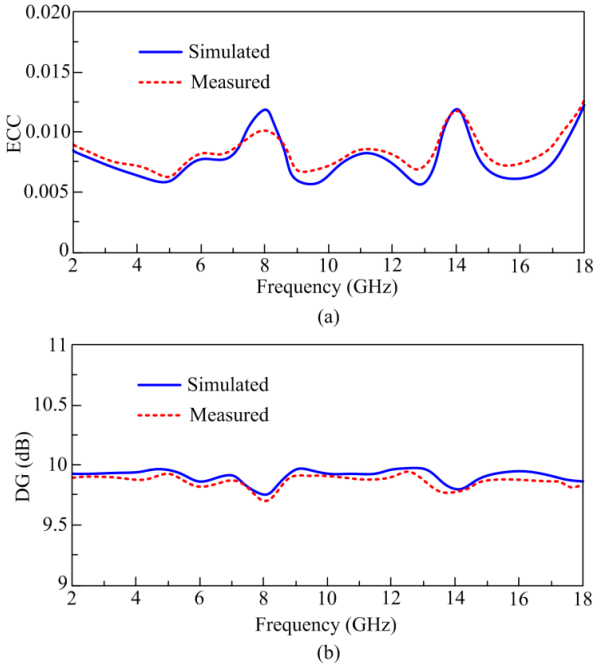

Fig. 19. The simulated and measured parameters of UWB MIMO antenna: (a) ECC and (b) DG.

V. CONCLUSION

In this work, a novel technique was developed to enhance isolation between two antennas in MIMO systems for 5G networks and IoT applications. This approach involved incorporating Split Ring Resonators (SRRs) between the MIMO elements, which led to excellent simulation results for interconnection. We analyzed various simulation parameters and constructed a physical system to measure factors such as S-parameters. The system demonstrated impressive diversity performance, with an envelope correlation coefficient (ECC) of less than 0.07 across the relevant frequency bands.The proposed design features four resonators arranged in an anti-parallel configuration, achieving over 17 dB isolation throughout the operating range. We evaluated both simulation and experimental data for gain, S-parameters, isolation, ECC, and radiation patterns. The results validate that using decoupling SRRs effectively reduces inter-element coupling and provides a strong diversity response. These findings suggest that the proposed MIMO antenna design is promising for ultra-wideband (UWB) applications. Future work could explore its potential in wireless communication systems, such as base station terminals.

ACKNOWLEDGMENT

This research was funded by Taif University, Saudi Arabia, Project Nº (TU- DSPP-2024-70).

REFERENCES

[1] G. Eason, B. Noble, and I. N. Sneddon, “On certain integrals of Lipschitz-Hankel type involving products of Bessel functions,” Phil. Trans. Roy. Soc. London, vol. A247, pp. 529–551, April 1955.

[2] V. Leithardt, D. Santos, L. Silva L. A solution for dynamic management of user profiles in IoT environments. IEEE Latin America Trans, Vol. 18, pp. 1193-1199, 2020.

[3] P. Kumar, T. Ali, M.M. Pai. Electromagnetic metamaterials: A pew paradigm of antenna design. IEEE Access, Vol; 9, pp. 18722–18751, 2021.

[4] W.A. Awan, A. Zaidi, N. Hussain, A. Iqbal, A. Baghdad. Stub loaded, low profile UWB antenna with independently controllable notch - bands. Microw Opt Technol Lett, Vol. 61, pp. 2447-2454, 2019.

[5] R.J Fontana. Recent system applications of short-pulse ultra-wideband (UWB) technology. IEEE Trans Microw Theory Techn, Vol. 52, pp. 2087–2104, 2004.

[6] J.Y. Siddiqui, C. Saha, C. Sarkar, L. A. Shaik, L.A, M.M.A. Yahia, Ultra-wideband antipodal tapered slot antenna with integrated frequency notch characteristics. IEEE Transactions on Antennas and Propagation, ,Vol. 66, pp. 1534-1539, 2018.

[7] S.C.Puri, S. Das, M.G. Tiary, UWB monopole antenna with dual-band-notched characteristics. Microw Opt Technol Lett, Vol. 62, pp. 1222–1229, 2020.

[8] E.M. Ali, W.A. Awan, M. S. Alizaidi, A. Alzahrani, D.H. Elkamchouchi, F. Falcone, S.S.M. Ghoneim. A shorted stub loaded UWB flexible antenna for small IoT devices. Sensors,Vol. 23, pp.748, 2023.

[9] FCC. FCC 1st report and order on Ultra-Wideband technology; FCC: Washington, DC, USA, 2002.

[10] A Zaidi, W.A. Awan, A. Ghaffar, M.S. Alzaidi, M. Alsharef, D.H. Elkamchouchi, S.S.M. Ghoneim, T.E.A. Alharbi. A low profile ultra-wideband antenna with reconfigurable notch band characteristics for smart electronic systems. Micromachines, Vol. 13, pp. 1803, 2022.

[11] M. Hussain, S. I. Naqvi, X. A. Awan, W.A.E. Ali, E.M. Ali, S. Khan, M. Alibakhshikenari. Simple wideband extended aperture antenna-inspired circular patch for V-band communication systems. AEU Int J Electron Commun, Vol; 144, pp. 154061, 2022.

[12] S. Lakrit, S.Das, A. El Alami, D. Barad, S. Mohapatra. A compact UWB monopole patch antenna with reconfigurable Band-notched characteristics for Wi-MAX and WLAN applications. AEU Int J Electron Commun, Vol. 105, pp. 106–115, 2019.

[13] M;A. Matin, Ultra-wideband current status and future trends; Intech Open: London, UK, 2012.

[14] S.A. Naqvi. Miniaturized triple-band and ultra-wideband (UWB) fractal antennas for UWB applications. Microw Opt Technol Lett, Vol. 59, pp. 1542–1546, 2017.

[15] W.A. Awan, D.M. Choi, N. Hussain, I. Elfergani, S.G. Park, N.A. Kim. frequency selective surface loaded UWB antenna for high gain applications. Comput Mater Contin, Vol. 73, pp. 6169-6180, 2022.

[16] S.G. Kirtania, B.A. Younes, A.R. Hossain, T. Karacolak, P.K. Sekhar. CPW-fed flexible ultra-wideband antenna for IoT applications. Micromachines, Vol. 12, pp. 453, 2021.

[17] W.A. Awan, S.I. Naqvi, N. Hussain, A. Ghaffar, A. Zaidi, X.J. Li, X. A Miniaturized UWB Antenna for Flexible Electronics. International Symposium on Antennas and Propagation and North American Radio Science Meeting, 2020, pp. 99-100.

[18] M.A. Sufian, N. Hussain, A. Abbas, W.A. Awan, D. Choi, N.A. Kim. Series fed planar array-based 4-port MIMO Antenna for 5G mmWave IoT applications. Asia-Pacific Microwave Conference (APMC), 2022, pp. 880-882.

[19] B. Yeboah-Akowuah, E.T. Tchao, M. Ur-Rehman, K.M. Khan, S. Ahmad. Study of a printed split-ring monopole for dualspectrum communications. Heliyon, Vol.7, PP; 7928, 2021.

[20] M.S. Alam, A. Abbosh. Reconfigurable band-rejection antenna for ultra-wideband applications. Microw. Antennas Propag. IET, Vol. 12, pp. 195–202, 2018.

[21] H. Abdi, J. Nourinia, C. Ghobadi. Compact Enhanced CPW-Fed Antenna for UWB Applications. Adv. Electromagn, Vol.10, pp. 15–20, 2021.

[22] A. Upadhyay, R.A. Khanna. CPW-fed tomb shaped antenna for UWB applications. Int. J. Innov. Technol. Explor. Eng. (IJITEE), Vol. 8, pp. 67–72, 2019.

[23] Z.A.A. Hassain, A.R. Azeez, M.M. Ali, T.A. Elwi. A modified compact bi-directional UWB tapered slot antenna with double band notch characteristics. Adv. Electromagn, Vol. 8, pp. 74–79,2019.

[24] P. Chaudhary, A. Kumar. Compact ultra-wideband circularly polarized CPW-fed monopole antenna. AEU Int. J. Electron. Commun, pp. 107, 137–145, 2020.

[25] X. P. Li, G. Xu, C.J. Duan, M.R. Ma, S.E. Shi, W. Li. Compact TSA with anti-spiral shape and lumped resistors for UWB applications. Micromachines, Vol. 12, pp. 1029, 2021.

[26] S. Kundu, A. Chatterjee. Sharp triple-notched ultra-wideband antenna with gain augmentation using FSS for ground pen-etrating radar. Wirel. Pers. Commun, Vol. 117, pp. 1399–1418, 2021.

[27] L. Guo, M. Min, W. Che, W. Yang. A novel miniaturized planar Ultra-Wideband antenna. IEEE Access, Vol. 7, pp. 2769–2773, 2018.

[28] A. Delphine, M. R. Hamid, N. Seman, M. Himdi. Broadband cloverleaf Vivaldi antenna with beam tilt characteristics. Int. J. RF Microw. Comput. Eng, Vol. 30, pp. 22158, 2020.

[29] M.M. Honari, M.S. Ghaffarian, R. Mirzavand. Miniaturized antipodal vivaldi antenna with improved bandwidth using exponential strip arms. Electronics, Vol. 10, pp. 83, 2021.

[30] W. Mu, H. Lin, Z. Wang, C. Li, M. Yang, W. Nie, J.A. Wu, flower-shaped miniaturized UWB-MIMO antenna with high isolation. Electronics, Vol. 11, pp. 2190, 2022.

[31] W. Zamir, D. Kumar. A compact 4 × 4 MIMO antenna for UWB applications. Microw. Opt. Technol. Lett, Vol. 58, pp. 1433–1436, 2016

[32] A.C. Suresh, T. Reddy. A Flower Shaped Miniaturized 4 × 4 MIMO Antenna for UWB Applications Using Characteristic Mode Analysis. Prog. Electromagn. Res. C, Vol. 119, pp. 219–233, 2022.

[33] V.R. Balaji, T. Addepalli, A. Desai, A. Nella, T.K Nguyen. An inverted L - strip loaded ground with hollow semi - hexagonal four - element polarization diversity UWB - MIMO antenna. Trans Emerging Telecommun Technol, Vol. 33, pp. 4381, 2022.

[34] R.B. Sadineni, P.G. Dinesha. Design of penta-band notched UWB MIMO antenna for diverse wireless applications. Prog Electromagn Res M, Vol. 107, pp. 35-49, 2022.

[35] B.T. Ahmed, I.F. Rodríguez. Compact high isolation UWB MIMO antennas. Wireless Networks, Vol. 28, pp. 1977-1999, 2022.

[36] G.A. Fadehan, Y. O. Olasoji, K.B. Adedeji. Mutual coupling effect and reduction method with modified electromagnetic band gap in UWB MIMO antenna. Appl. Sci, Vol. 12, pp. 12358, 2022.

[37] C.A. Balanis, Antenna theory: analysis and design. John wiley & sons, 2015.

[38] W.A. Awan, S.I. Naqvi, A.H. Naqvi, S.M. Abbas, A. Zaidi, N. Hussain. Design and characterization of wideband printed antenna based on DGS for 28 GHz 5G applications. J Electromagn Eng Sci, Vol. 21, pp. 177-183, 2021.

[39] N. Hussain, W.A. Awan, W. Ali, S.I. Naqvi, A. Zaidi, T.T. Le. Compact wideband patch antenna and its MIMO configuration for 28 GHz applications. AEU Int J Electron Commun, Vol. 132, pp. 153612, 2021.

[40] M. Alibakhshi-Kenari, M. Khalily, B.S. Virdee, C. See, R. Abd-Alhameed, E. Limiti. Mutual Coupling Suppression Between Two Closely Placed Microstrip Patches Using EM-Bandgap Metamaterial Fractal Loading, IEEE Access, 2019, Vol. 7, pp. 23606 – 23614, 2019.

[41] M. Alibakhshi-Kenari, M. Khalily, B.S. Virdee, C. See, R. Abd-Alhameed, A.H. Ali, F. Falcone, E. Limiti. Study on Isolation Improvement Between Closely Packed Patch Antenna Arrays Based on Fractal Metamaterial Electromagnetic Bandgap Structures, IET Microwaves, Antennas & Propagation , Vol. 12, p. 2241 – 2247, 2018.

[42] H. Xiong. J. Li, J. S. He. High isolation compact four-port MIMO antenna systems with built-in filters as isolation structure", Proceedings of the Fourth European Conference on Antennas and Propagation (EuCAP) 2016, pp. 1-4.

[43] I. Dioum. Conception de systèmes multi-antennaires pour techniques de diversité et MIMO -Application aux petits objets nomades communicants, Thèse de Doctorat, Université de Nice Sophia Antipolis, Ecole doctorale sciences et technologies de l'information et de la communication , 2016.

[44] J.G. Joshi, S.S. Pattnaik, S. Devi, M.R. Lohokare, M.R. Microstrip Patch Antenna Loaded with Magneto inductive Waveguide", 12th National Symposium on Antennas and Propagation 2010, pp.101-105.

[45] M. Alibakhshi-Kenari, B.S. Virdee. Study on Isolation and Radiation Behaviours of a 34×34 Array-Antennas Based on SIW and Metasurface Properties for Applications in Terahertz Band Over 125-300 GHz", Optik, International Journal for Light and Electron Optics, vol. 206, 2020.

[46] A. Chebihi, C. Luxey, A. Diallo, A. Le Thuc, R. Staraj. A Novel Isolation Technique for Closely Spaced PIFAs for UMTS Mobile Phones", IEEE Antennas and Wireless Propagation Letters, vol. 7, pp. 665-668,2008.

[47] S.C. Hwang, R.A. Abd- Alhameed, Z. Z. Abidin, N.J. Mc Ewan, P.S. Excell. Wideband printed MIMO/diversity monopole antenna for WiFi/WiMAX applications," IEEE Trans. on Antennas and Propagation, vol. 60, pp. 2028-2035, 2012.

[48] X.Q. Lin, H. Li, S. He, Y. Fan, A decoupling technique for increasing the port isolation between two closely packed antennas", 2012 IEEE Antennas and Propagation Society International Symposium (APSURSI), 2012, pp. 1-2.

[49] S. Luo, Y. Chen, D. Wang, Y. Liao, Y. Li. A monopole UWB antenna with sextuple band-notched based on SRRs and U-shaped parasitic strips. AEU-Int. J. Electron. Commun, Vol. 120, pp. 15, 2020.

[50] B. Ajewole, P. Kumar, T. Afullo, I-Shaped Metamaterial Using SRR for Multi-Band Wireless Communication, Crystals, Vol.12, pp. 559, 2022.

[51] R.B. Rani, S.K. Pandey. A CPW-fed circular patch antenna inspired by reduced ground plane and CSRR slot for UWB applications with notch band, Microw. Opt. Technol. Lett. vol. 59, pp. 745–749, 2017.

[52] N. Sharma, S.S. Bhatia. Metamaterial Inspired Fidget Spinner-Shaped Antenna Based on Parasitic Split Ring Resonator for Multi-Standard Wireless Applications. J. Electromagn. Waves Appl, Vol. 34, pp. 1471–1490, 2020.

[53] R. Mark, N. Rajak, K. Mandal, S. Das. Metamaterial based superstrate towards the isolation and gain enhancement of MIMO antenna for WLAN application. AEU, Int. J. Electron. Commun, vol. 100, pp. 144–152, 2019.

[54] F.B. Zarrabi, Z. Pirooj, K. Pedram, Metamaterial loads used in microstrip antenna for circular polarization, Int J RF Microw Comput Aided Eng, Vol. 29, pp. 21869, 2019.

[55] R. Mark, N. Rajak, K. Mandal, S. Das, S. Metamaterial based superstrate towards the isolation and gain enhancement of MIMO antenna for WLAN application. AEU, Int. J. Electron. Commun, vol. 100, pp. 144–152, 2019.

[56] M. Hussain, W.A. Awan, E.M. Ali, M.S. Alzaidi, M. Alsharef, D.H. Elkamchouchi, A. Alzahrani, M. Fathy Abo Sree. isolation improvement of parasitic element-loaded dual-band MIMO antenna for Mm-Wave applications. Micromachines 2022, 13, 1918.

[57] Bayarzaya, B.; Hussain, N.; Awan, W.A.; Sufian, M.A.; Abbas, A.; Choi, D.; Lee, J.; Kim, N. A compact MIMO antenna with improved isolation for ISM, Sub-6 GHz, and WLAN application. Micromachines , Vol. 13, pp. 1355, 2022.

[58] H. Khalid, W.A. Awan, M. Hussain, A. Fatima, M. Ali, N. Hussain, S. Khan, M. Alibakhshikenari, E. Limiti. Design of an integrated sub-6 GHz and mmWave MIMO antenna for 5G handheld devices. Appl. Sci., Vol. 11, pp. 8331, 2021.